Biomedical Sensors and Their Interfacing

Rajarshi Gupta

Abstract Biomedical sensors provide an interface between the electrophysiological activity of different body organs and the instruments those facilitate an in-depth analysis of the pathological conditions. They constitute the most important part of a biomedical health monitoring system. Electrocardiogram (ECG), Photoplethysmogram (PPG), Blood pressure (BP) and respiration are the most fundamental cardiac and respiratory function indicators in a human body. This chapter is aimed to provide a brief overview of these sensors and interfacing techniques for digitized acquisition.

1 Introduction

Many organs in the human body, such as the heart, the brain, muscles, and eyes, have underlying electrophysiological activities and involve generation of electric fields and small biopotentials. Measurements of these and other bio-electric signals can provide information on normal or pathological functions of the organs. The fundamental objective of any medical signal acquisition system is to faithfully capture the information which represents the physiological event or phenomena using a suitable sensor. Over the years, various types of medical sensors have been developed using the principles of materials science, electrical engineering, and electronics science. Historically, the earliest uses of these sensors were confined to clinical use, mainly in hospitals and healthcare clinics. However, with the ever-changing societal demands (busy work schedule of common people) as well as application of medical technology to non-medical domain (space application, sports physiology, military applications, smart home systems to name a few), there were requirements to access medical data remotely, using portable systems (handheld gadgets) and also at the mobile condition of the subject (patient). These demanded

R. Gupta (✉)
Department of Applied Physics, Instrumentation Engineering,
University of Calcutta, Calcutta, India
e-mail: rgaphy@caluniv.ac.in

B. George et al. (eds.), *Advanced Interfacing Techniques for Sensors*,
Smart Sensors, Measurement and Instrumentation 25,
DOI 10.1007/978-3-319-55369-6_7

contribution from embedded technology, information and communication technology, computer science into the broad area of biomedical engineering. The technological challenge in this area in the current century is primarily two fold. First, development of lightweight, miniature and wearable sensors so that medical signals can be acquired from a patient even during his normal daily activity. Second, use of wireless senor networks, embedded technology, and computing tools for continuous monitoring of patients for early detection of pathological events from medical signal(s). Among the various medical signals, cardiovascular signals are considered the most important ones. The frequently used cardiovascular signals, viz., Electrocardiogram (ECG), peripheral pulse, blood pressure (BP) and respiration provide an in-depth assessment of the organs like heart, lungs, and circulatory system. The scope of this chapter is to discuss the basic sensing principles and interfacing of these cardiovascular and respiration sensors for their digitized acquisition in a processor based system. These signals are also functionally and physiologically interrelated in the sense that a pathological symptom obtained in one signal can be sometimes clinically correlated to the other one(s). The layout of the chapter is as follows: Sect. 2 discusses the fundamental bioelectric phenomena underlying the origin of physiological signals and requirements of any medical signal acquisition system. In Sect. 3, basic origin of the cardiovascular and respiratory signals is discussed in brief. Section 4 is dedicated for signal conditioning circuits and interfacing of these signals, followed by a discussion on wireless biomedical instrumentation in Sect. 5. Section 6 highlights two recent developments of modern medical sensors. For the curious and enthusiastic readers, end of chapter references will help to get comprehensive information on the pertinent areas in detail.

2 Basic Aspects of Biomedical Data Acquisition Systems

Biomedical signals, according to their sources and acquisition principles, are divided into two broad classes, viz. (a) endogenous signals and (b) exogenous signals. The endogenous signals arise from natural physiological processes (hence, also called physiological signals) and are measured within or on living creatures. Example of such signals are EEG, ECG, EMG, EOG, blood glucose; etc. The exogenous signals arise from the modulation of an externally applied energy or radiation onto a physiological organ. The external energy or radiation may be of suitable wavelength, X-ray, ultrasound energy, magnetic field etc. Examples of such signals are PPG, SpO_2, blood pressure etc. While endogenous signals can be acquired invasively or non-invasively, exogenous signals are mostly drawn non-invasively.

The sources of nearly all physiological signals may be attributed to the transients in intercellular membrane potentials known as resting membrane potentials (RMP) in excitable living organisms [1, 2]. The electrophysiological basis of generation of such tiny potentials is due to the fact the living cells undergo a

reversible change due to an external stimulation. The asymmetric distribution of Na^+, K^+, Ca^{++}, and Cl^- ions which are the principal constituents of intra and extra cellular fluids and semi-permeable nature of the membrane gives rise to the RMP. The RMP of most human living cells is around −20 to −70 mV while measured inside to outside of the cell membrane. The steady state RMP was represented by Goldman–Hodgkin–Katz equation [3]:

$$V_{mo} = -\frac{RT}{F}\left\{\frac{[Na^+]_i P_{Na^+} + [K^+]_i P_{K^+} + [Cl^-]_i P_{Cl^-}}{[Na^+]_e P_{Na^+} + [K^+]_e P_{K^+} + [Cl^-]_E P_{Cl^-}}\right\} \quad (1)$$

where, T is the Kelvin temperature, R is the MKS gas constant (8.314 J/(mol K)), F is the Faraday number, 96,500 Cb/mol, and P_X is the permeability for ion species X.

This 'polarized' behaviour cell of the cell gets changed due to application of short duration external stimulus. An 'ion pump' theory describes the movement of ions through the cell membrane which makes the cell potential rapidly reversed for some time, called 'depolarization' of the cell. After the stimulus is withdrawn, it slowly recovers to the initial polarized state through a slow 'repolarization' and occasional after-potentials. The recording of the membrane potential during these reversible changes is called action potential of the cell, the magnitude, shape and duration of which depends on the type of cell, like nerve, muscle or cardiac [3].

The recording of any physiological signal is the collective representation of these tiny action potentials over space and time at predefined body location(s). The basic aspects of any medical signal acquisition system are [4]:

(a) Sensing of very weak amplitudes, since most biopotentials appear in the order of millivolt or microvolt signal at the body surface. This requires that the sensing electrodes should be sensitive enough to capture these weak biosignals.
(b) Removal or minimization of unwanted signals, collectively named as noise and artifacts, which can be external (interferences from power line, radiofrequency sources, amplifier noise etc.) or internal (physiological signals from other body tissues). If not minimized, these can corrupt the desired medical signal completely, making it either unacceptable for clinical diagnosis or prone to wrong diagnosis.
(c) Safety of the subject (patient) from (i) electrical power supply of medical instrument; (ii) radiation energy imparted on the patient for exogenous signals (for imaging applications), and (iii) any other toxic materials or effects in the process of signal acquisition.
(d) Presentation of the signal in an acceptable format or standard that is suitable for interpretation by the medical experts. This mainly refers to the protocols or standard lead configurations for acquisition of different medical signals, for example, 12-lead ECG for Electrocardiograms.

3 Cardiovascular and Respiratory Signals: Origin and Basic Principle

Cardiovascular and respiratory signals arise from the pumping actions of the heart in conjunction with the circulatory systems that supply the blood to each body cell and, inhalation and exhalation of air to purify the blood through pulmonary circulation, respectively. The signals which represent proper functioning of these two systems are, ECG, peripheral pulse (also known as digital volume pulse or Photoplethysmogram), saturated oxygen in blood (SpO_2), systolic and diastolic BP and respiration.

3.1 Electrocardiogram Signal

The Electrocardiography (EKG or ECG) is the prime investigation tool for preliminary level cardiac functions. It represents time averaged representation of the tiny electrical potentials generated at the sinoatrial (SA) node of the heart and their propagation along specialized conduction fibers over the heart's surface, as recorded at predefined body positions. As shown in Fig. 1, a typical ECG waveform consists of P, QRS and T waves, which represent sequential depolarization and repolarization of the atrial and ventricular myocardium cells [5]. Among these, the P-wave is represented by atrial depolarization during which the electric pulses move from SA node to atrio-ventricular (AV) node, where the conduction is delayed to form the equipotential PQ segment. This is followed by spreading of electric conduction pulses through bundle of His, left bundle branch and right bundle branch along the ventricular region, representing its depolarization to generate QRS complex which suppresses the simultaneous atrial repolarization. A little time pause here gives rise to equipotential ST segment, after which ventricular repolarization

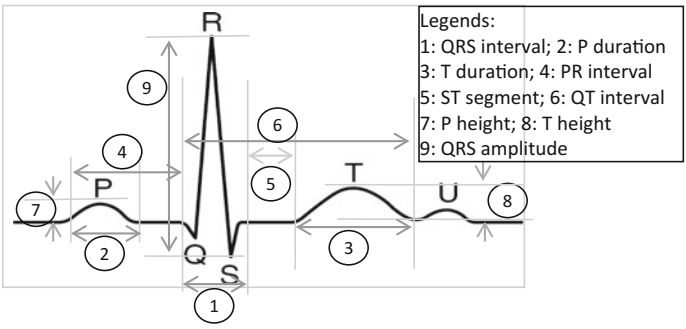

Fig. 1 A typical representative ECG beat in important clinical features (printed from "Hybrid Encoding for Real Time Compressed Electrocardiogram Acquisition", Measurement, Vol. 91, Sept. 2016, (Elsevier Sc.) by P. Bera et al. with permission)

starts with conduction pulses spreading over Purkinjee fibers, with generation of T wave. The important clinical features (marked as 1–9 in Fig. 1) that describe the cardiac function lies in the different time durations and amplitudes of constitutes waves and wave segments. These provide a set of quantitative and qualitative (curvature of a wave, elevation or depression of a segment etc.) metrics which provide a foundation of objective assessment by a cardiologist [6, 7]. A lot of cardiac disorders like arrhythmia, ectopic beats, myocardial infarction, hypertrophy, bundle branch block etc. can be detected by visual analysis or computerized analysis of such features or their suitable combination [8].

'12-lead ECG', an internationally accepted standard for recording of ECG in clinical practice, represents body positions and referencing system to record ECG. Left arm, right arm and left leg are used for recording three standard bipolar leads I, II and III and three unipolar augmented limb leads aVL, aVR, and aVF. Six unipolar chest leads v1, v2, v3, v4, v5 and v6 are attached to different intercostals spaces on the rib-cage. For unipolar leads, the reference is taken as the Wilson Central Terminal (WCT). With the advent of computerized recording and analysis, these 12—lead traces can be simultaneously acquired and analysed to provide preliminary level assessment of cardiac abnormality.

3.2 Peripheral Pulse Signal

Peripheral pulse signal can provide vital diagnostic information on blood circulatory functions through the veins and arteries spread over the whole body. They represent blood volume changes in the micro vascular bed of tissue at the peripheral body parts (like fingertips, earlobes, and forehead) with respect to a cardiac cycle. The most popular technology to acquire such signals is photoelectric plethysmography or, Photoplethysmography (PPG) [9, 10]. Here, an optical source-detector combination attached to the body part is used to illuminate a small portion of skin and sense the change in blood volume information based on difference of absorbance of the light radiation between blood-full and blood-less skin at near infrared (IR) wavelengths. The sensor electronics projects this change in the output voltage. A typical PPG waveform shows a steady (DC) component (representing thermoregulation and autonomic functions), and a pulsatile component (representing blood volume changes). As shown in Fig. 2, the rising part of the pulsatile component is called anacrotic phase, and it represents ventricular systole (contraction), where the supply of blood to the peripheral capillary increases. It is characterized by the systolic peak (point SP), after which the falling part, named catacrotic phase starts, representing ventricular diastole (expansion). For healthy arterial condition, a diastolic peak (point DP) reflects momentary rise in blood supply due to reflection of pulse wave pressure from the closed aorta. Like ECG, PPG also provides a set of objective measurements based on its morphological features, as indicated in Fig. 2. A multitude of cardiovascular parameters like heart rate, cardiac output, respiration, endothelium functions, arterial compliance, and

Notation	Description
amplitude (F-SP)	Systolic amplitude (SA)
duration (h1-h2)	Pulse width (PW)
duration (SP-DP)	Peak to peak time (PPT)
duration (F-SP)	Crest Time (CT)
amplitude (F-DN)	Dicrotic notch amplitude (DNA)
amplitude (F-DP)	Diastolic peak amplitude (DA)
Ratio (SA/DA)	Augmentation index (AI)

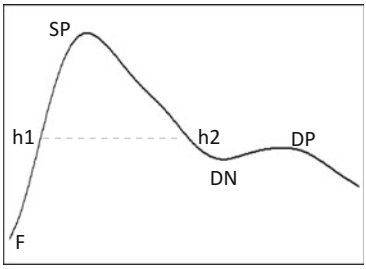

Fig. 2 A finger pulse waveform representing main clinical features

blood pressures can be correlated from the PPG and ECG-PPG combination [11–16]. Over the last two decades, an increase in interest in PPG technique by the biomedical research community has raised its use for various clinical monitoring purposes due to its non-invasive acquisition, low cost instrumentation, single site measurement and favourable sensor configuration [17, 18].

Notation	Description
Amplitude (F-SP)	Systolic amplitude (SA)
Duration (h1-h2)	Pulse width (PW)
Duration (SP-DP)	Peak to peak time (PPT)
Duration (F-SP)	Crest time (CT)
Amplitude (F-DN)	Dicrotic notch amplitude (DNA)
Amplitude (F-DP)	Diastolic peak amplitude (DA)
Ratio (SA/DA)	Augmentation index (AI)

3.3 Respiration Signal

The objective assessment of lungs, airways and chest wall functionality can be made by direct or indirect measurement of various variables which are associated with two key events in the respiratory system, viz., transport of the gas from environment and the alveoli via the branching airway tree, and, diffusion of the gases across the physical barrier separating the alveoli from the pulmonary capillaries. The various measurements under the respiration system can be classified under the following heads: (a) gas pressure; (b) gas flow and volume; (c) concentration and partial pressure of gases; (d) pulse oximetry and capnography; (e) lung mechanical function (spirometry and body plethysmography) and, (f) gas exchange [19]. In this chapter, discussion is confined to airflow sensing and breathing rate measurements using plethysmography.

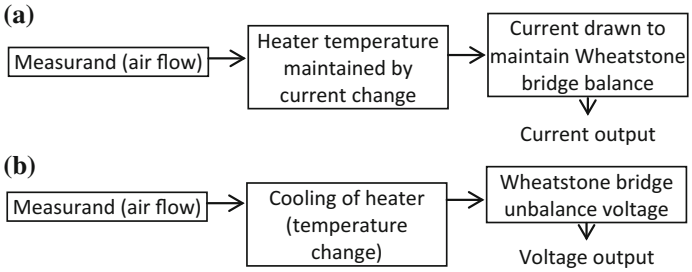

Fig. 3 Basic principle of thermal convection flow meters: **a** Constant temperature mode. **b** Constant current mode

Thermal convection flow meters employing sensing elements like (electrically heated) metal wires, metal films, and thermistors are used to measure gas flow rate through the nasal cavity and provides indirect measurement of respiration in terms of lung volume or its changes [20]. These thermal flow sensors are based on convective heat exchange that takes place when the fluid flow passes over the sensing element (hot body). They are connected in a full Wheatstone bridge and normally designed to operate either in constant temperature mode or, in constant current mode. The basic sensing principle is shown in Fig. 3. The airflow due to breathing activity takes away the heat from the sensing element. In constant temperature mode, the heater element is maintained at constant temperature by adjustment of current from the source, whereas in constant current mode, the heater is supplied with constant current and bridge unbalance provides a measure of air flow rate.

A popular form of respiratory air flow sensing is employing **microwave Doppler radar** [21–23] which avoids sensor attachment, or special clothing, and provides additional advantages like robustness against environmental factors, interference from other sensor signals etc. The sensor operates by transmitting a radio wave (typically in the GHz range) signal and receiving the modulated version of the signal due to quasi periodic motion of the chest wall/abdomen due to inhalation, exhalation and the pause in between.

Plethysmography is a general technique used for measuring respiration, or breathing effort by change in volume (abdominal or chest sectional area). The basic configuration employs change in elastic belt tension (piezo or strain gauge as sensing element), electrical impedance (change in current between two electrode positions) and inductive type (frequency change in a RF signal looped in a chest belt) [24–26]. Among these, chest belt type respiratory inductive plethysmography (RIP) sensors are popular and often taken as standard to calibrate other respiration sensors. In RIP [27], a low current is looped through a coil would around the chest and activated by a high frequency (~kHz) current source. As a result of quasi-periodic motion of chest and abdomen, the body sectional (chest) area changes and so changes the resultant magnetic field. This can be measured by change in frequency in the loop current.

3.4 Blood Pressure Signal

Blood pressure (BP) is the pressure exerted by the circulating blood in the walls of the peripheral vascular system and different chambers of the heart. BP measurement is a standard clinical practice and gives a rough estimation of the integrity of the cardiovascular system. Measurement of BP mainly aims to determine the systolic pressure (when the ventricles contract), diastolic pressure (when the ventricles expand) and mean arterial pressure [28]. The Association for the Advancement of Medical Instrumentation (AAMI) demands a pressure range of –30 to 300 mmHg for a blood pressure transducer. Additionally, it should not be damaged with an overpressure in the range of –400 to 4000 mmHg.

There are several direct and indirect methods for measuring BP. Direct BP measurements involve minor surgical procedure to couple the (body) site pressure to an external sensor, and categorized into extravascular and intravascular sensors. These are applied for pre-and post-surgical patients under hospital set up. Modern electrical type direct BP measurement methods adopt 'catheterization' techniques, which detect deflection of an elastic member by the exerted pressure. The secondary sensing principle may utilize strain gage, piezoelectric, capacitive or fiber optic principles and mostly of intravascular type.

In routine clinical check-ups, however, indirect BP measurements (non-invasive) employ an inflated cuff by air purging for occlusion of a blood vessel (normally brachial artery). In general, the cuff is inflated above the tentative systolic BP and slowly bled off at a rate of 2–3 mm/Hg. With gradual release of cuff pressure, blood leaks through the occluded artery. Based on the sensing principle, the measurement methods are categorized into auscultation, palpation, flush and oscillometric techniques [4, 29, 30]. The auscultation method uses a stethoscope to hear the appearance and disappearance of different phases of Korotkoff sounds with the gradual decreases of cuff pressure. Several improvisations of the auscultation methods facilitate automated detection of systolic and diastolic BPs by employing secondary transducers like piezo crystals, ultrasonic, photoelectric, and electroacoustic transducers. The palpation of the radial artery with gradual release of the cuff pressure can be manually sensed to detect the systolic pressure only. The oscillometric method measures the amplitude of oscillations that appear in the cuff pressure signal created by the arterial wall as the blood leaks through the brachial artery. This method can provide systolic, mean and diastolic (using algorithm) pressures. In the last two decades, several sensor designs and computational methods have been proposed for indirect BP measurement using ECG and PPG [31–33]. These have opened up a new domain of non-invasive [34], continuous and ubiquitous cardiovascular measurements.

4 Sensor Configurations and Interfacing of Cardiovascular and Respiratory Signals

Most of the real world biomedical signals are weak in amplitude (order of millivolt or microvolt) and so, require amplification, scaling, isolation and filtering before being finally acquired in a collecting device. These functions are collectively known as signal conditioning. The biomedical sensors are interfaced with the signal conditioning circuits at the first stage of recording. Among these, filtering is used to pass the clinical bandwidth of the signal and discard any noise from the raw input. Isolation is a special function used for endogenous medical signals (like ECG, EMG). The signal conditioning circuit configuration depends on the biomedical signal being acquired and provides an amplification from 10–10^6 to the raw input.

4.1 Electrocardiogram Signal

The ECG is measured from the predefined positions of human body. However, for its proper measurement electrodes are required which convert the ionic current (inside the body) to the electronic current in an external circuit, i.e., the measurement electronics. Apart from that, ECG signals being weak in magnitude (±3 mV peak), they are inherently corrupted by other physiological signals (like muscle noise) and external unwanted interferences, collectively known as 'artifacts'. Hence, proper filtering, amplification and isolation are required for its proper recording, presentation and safety of the patient.

The block diagram of a typical ECG signal conditioning is shown in Fig. 4, which can generate a unipolar voltage. The lead selector circuit can be manually operated or controlled by the data acquisition (DAQ) board.

The objective of the isolation circuit is to provide galvanic isolation (1000 MΩ or more) between the patient body and the signal conditioning to prevent any accidental current flowing through the patient body. The total gain of the amplifier is around 2000, distributed over a pre-amplifier and an instrumentation amplifier (INA). The first stage, pre-amplifier provides a low gain, typically 10–20. The filter circuit mainly discards high frequency noise and passes the clinical bandwidth of 0.05–100 Hz to the output. The INA provides a gain of 100–200. After INA, the

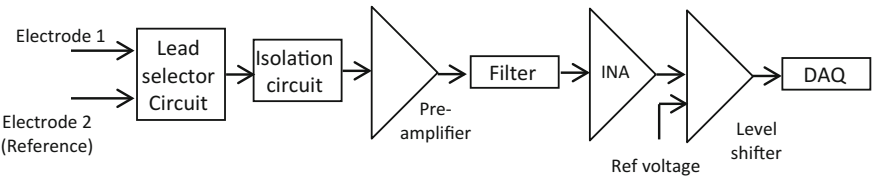

Fig. 4 Block schematic of a ECG amplifier circuit

final level shifter is used to get a unipolar voltage 0–5 V. In the following sections, the components of the ECG signal conditioning are elaborated.

4.1.1 Electrodes

Electrodes facilitate conversion of the ionic current within the body tissue to an external current using a metal-electrolyte interface. Electrodes are categorized into polarized and non-polarized according to their electrical behaviour. A detailed analysis of the biopotential electrodes are available in [2, 4]. Silver-Silver Chloride electrodes provide the most stable performance. They are made of silver disks coated electrolytically by silver chloride. The electrolyte (gel) additionally provides protection against slippage of the electrodes. Commercially, two types of electrodes are used in ECG recording, viz., reusable and disposable.

Figure 5 shows common electrodes used for ECG recording. Here, (a), (b) and (c) are metal reusable electrodes used in common clinical settings. Materials used for these types of electrodes include German silver (a nickel-silver alloy), silver, gold, and platinum. Among these, (a) is a suction cup electrode for precordial or chest leads. The (b) type is used as limb electrode. The type (c) is a general metal disc electrode which is normally used in long-term ECG recording. A lead wire is soldered into the back surface for electrical connection to recorder. A thin insulating material epoxy or polyvinylchloride protects the conducting part from lead wire. (d) Shows another reusable Silver-Silver Chloride electrode attached to the skin by non-allergic adhesive tape, and provides high quality measurement. (e) and (f) are disposable electrodes used in research due to their improved design. Configuration (e) provides a secure arrangement by attaching a large foam pad to the electrode

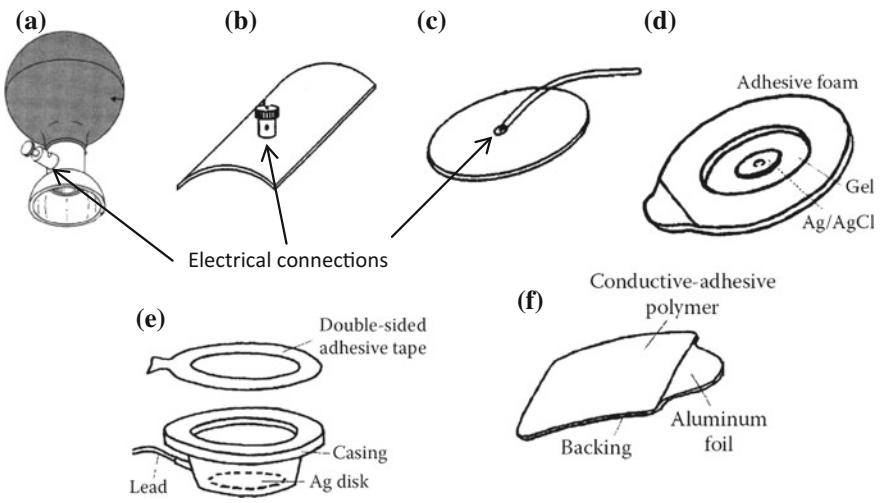

Fig. 5 Some electrodes used for ECG acquisition

body with adhesive coating on one side. The gel is trapped in the pocket between the electrode contact surface and skin. A double sided adhesive tape fixes the electrode on one side, and the body surface on the other. Such electrodes are particularly suited in ambulatory recordings for long term use. Configuration (f) shows special conductive polymer electrodes developed in recent times, with the advantage of conducting and adhesive properties simultaneously. The polymer is attached to a metallic backing made of silver or aluminum foil, allowing electric contact to external instrumentation.

4.1.2 Isolation Circuits

According to guidelines from AAMI, all medical amplifiers must comply with certain safety standards. Among them, one important is IEC 60601-1 standard, which prescribes a limiting patient auxiliary current (current that can flow between two separate leads connected to the patient body) up to 100 μA at 0.1 Hz. The isolation between the patient and the electrical recorder is achieved in two ways. First, complete galvanic isolation using optical, capacitive or magnetic coupling between the recording leads and amplifier inputs. Second, using surge protection arising from electrosurgical equipments or defibrillators [35].

In magnetic isolation, a transformer is used to achieve nearly 7 kV of isolation between the primary and secondary. The low frequency ECG signal modulates a high frequency carrier (around 500 kHz) signal, and transferred to secondary through magnetic coupling. At the output, a demodulator (low pass filter) extracts the ECG. This is schematically shown in Fig. 6a.

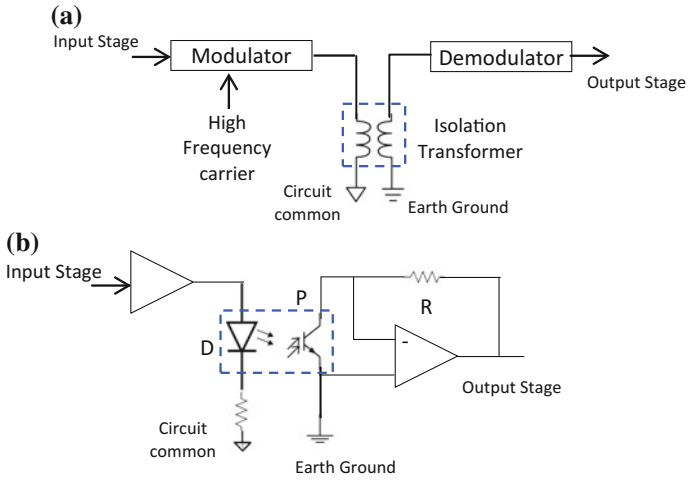

Fig. 6 Different types of isolation strategy in ECG amplifiers: **a** magnetic isolation. **b** Optical isolation

An optical isolation amplifier uses a linear opto-coupler using infrared LED and a phototransistor to separate the input and output (Fig. 6b).

4.1.3 Filtering Circuits

Among the major artifacts which corrupt the ECG signal are electromyography noise, baseline wander, motion artifacts, power line interference (PLI), electrode pop or contact noise, baseline wander, electrosurgical noise, and amplifier noise [8]. Some of these artifacts have overlapping spectra with the ECG, and hence only filtering in analog domain may not be sufficient for their complete removal. However, for practical purposes, a band pass filter in the frequency range 0.05–70 Hz can remove most of the artifacts, except PLI. Two filtering circuits at the first stage (pre-amplifier) are shown in Fig. 7. In (a), small ferrite beads (T1) and inductors at the lead wires, along with a low pass filter using R_0 and C_0 can substantially reduce the high frequency electromagnetic and radio frequency interference. A band pass filter using the R_1, C_1 and R_2, C_2 combination can select the clinical bandwidth of ECG using band pass filter, with the pass band given by:

$$f = \frac{1}{2\pi}\left(\frac{1}{R_1 C_1} - \frac{1}{R_2 C_2}\right) \tag{2}$$

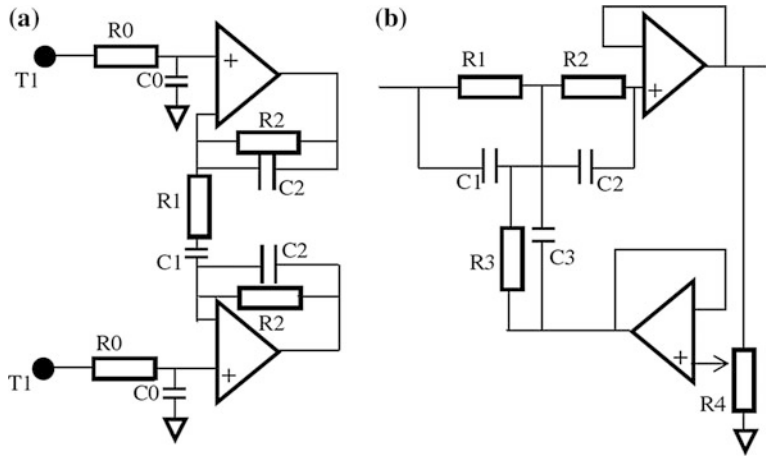

Fig. 7 Filtering circuit for noise reduction: **a** band pass filtering; **b** power line interference (printed from "ECG Acquisition and automated remote processing", (Springer, 2014) by R. Gupta et al. with permission)

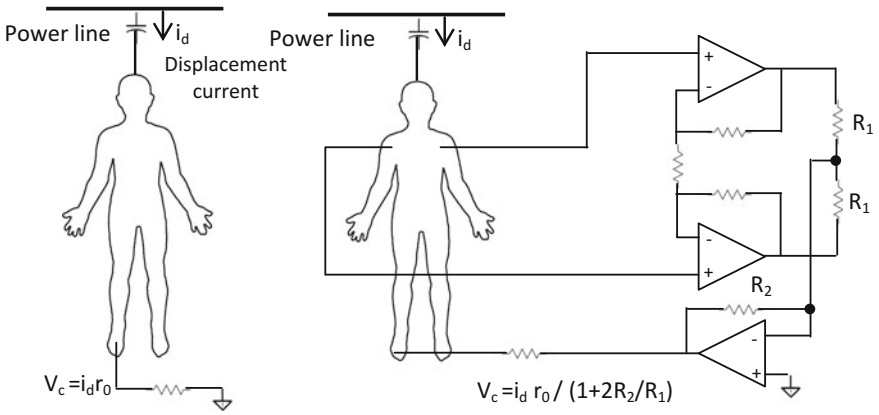

Fig. 8 Power line interference reduction using driven *right* leg circuit (printed from "ECG Acquisition and Automated Remote Processing", (Springer, 2014) by R. Gupta et al. with permission)

A twin T notch filter, shown in (b) can minimize the PLI. The rejected frequency is given as:

$$f = \frac{1}{2\pi R_1 C_1} \tag{3}$$

where, $R_1 = R_2 = 2R_3$; $C_1 = C_2 = C_3/2$.

Another improvisation to minimize power line noise is to use driven right leg circuit, frequently used in commercial ECG recorders and research equipments. The right leg of the subject is used as reference for unipolar lead ECG measurements. A feedback circuit from the first stage (pre-amplifier) output using a voltage divider can reduce the PLI, as shown in Fig. 8. Stray electrical capacitances are formed with the patient body, lead wires and the power line. The induced displacement current i_d creates a common mode voltage ($V_0 = i_d \times r_0$) at the lead wires (having resistance r_0) which, at power line frequency can be as high as 20 mV. The DRL circuit uses a feedback amplifier to reduce this common mode voltage to:

$$V_c = \frac{i_d r_o}{1 + \frac{2R_2}{R_1}} \tag{4}$$

Here, by proper choice of R_2 the PLI effect can be minimized.

4.1.4 Instrumentation Amplifier (INA)

An ECG INA should have some basic characteristics for faithful amplification of the low amplitude signal. The most essential of them are: high common mode

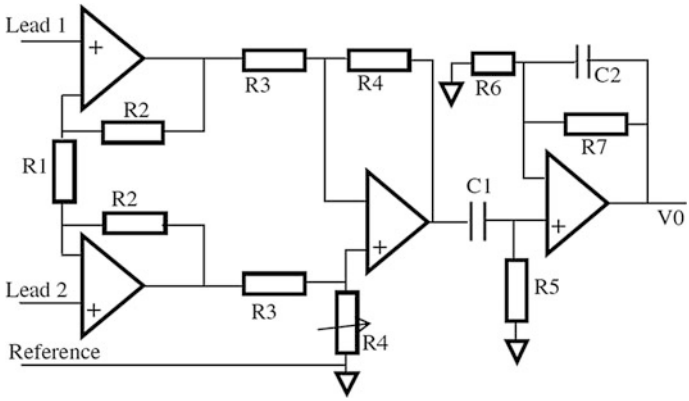

Fig. 9 Three OPAMP classical ECG amplifier configuration (printed from "ECG Acquisition and automated remote processing", (Springer, 2014) by R. Gupta et al. with permission)

rejection (CMR) and high input impedance. The CMR at the first stage (pre-amplifier) is one prime factor to minimize the noise generated from PLI as well as potential arising out of electrode-skin interface, which can saturate the output of the final amplifier. A typical CMR ratio of 250–300 dB and input impedance of 100 MΩ at 60 Hz can provide good results. Apart from these, the amplifier should have a good 'recovery' property which enables it to track the input after saturation due to sudden movement of the patient during ECG procedure. A modified configuration of classical three-OPAMP circuit is shown in Fig. 9 [8], where the total gain is distributed among the three stages, given by:

$$G = (1 + \frac{2R_2}{R_1})(\frac{R_4}{R_3})(1 + \frac{R_7}{R_6}) \tag{5}$$

This design also offers a band pass filter in the final stage:

$$\Delta f = \frac{1}{2\pi}(\frac{1}{R_7 C_2} - \frac{1}{R_5 C_1}) \tag{6}$$

Some low power monolithic INA designs are available in [36, 37]. AD620 from Analog Instruments is used in some ECG amplifier designs in recent times. This IC has some attractive features, like, using a single external register (R_G) to achieve a gain in the range 1 to 10^3, very good CMRR of 100 dB at gain of 10, low operating voltage 2.3 V, which outperforms a classical three-OPAMP IA circuit for ECG amplifiers.

A practical ECG amplifier (without the isolation stage) with AD620 is shown in Fig. 10. The circuit consists of four stages. In the first stage AD620 provides low gain, typically 10–15 and high CMRR. The filter at this output can prevent the saturation due to electrode offset voltage. The second stage (CA3140) implements a

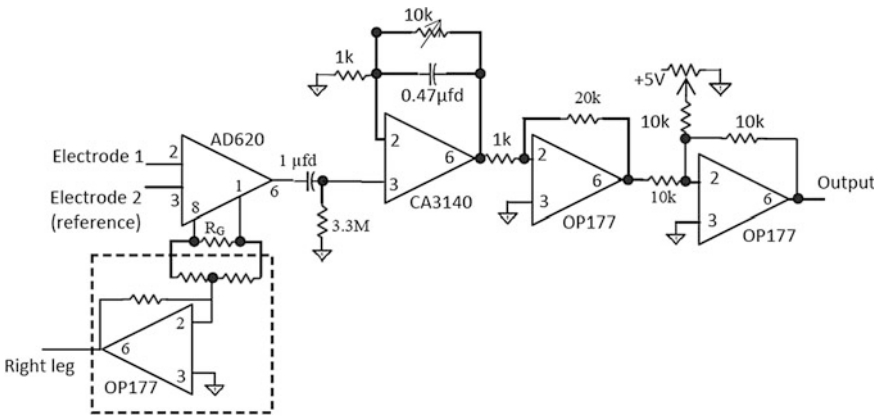

Fig. 10 Practical ECG amplifier using AD620

low pass filter of 70 Hz cutoff and a gain of 10. The third (OP177) stage, a simple inverting amplifier, provides a gain of 20. The final OP1-177 provides an adjustable bias to get unipolar final output. This design also implements driven right leg circuit.

4.2 Peripheral Pulse Signal (Photoplethysmogram)

There are two configurations of PPG sensors, viz., transmission mode, and, reflectance mode. The transmission type is more common in use and can be applied in peripheral body parts. In this mode a matched pair of LED and photodiode is attached to opposite surface of body extremity. In the 0.8–1 μm wavelength (named optical water window), the light is least absorbed by the water content of the tissue. A pulse of blood in the illuminated capillary increases the optical density, and there is a decrease in received light intensity at photodiode. The absorption is quantitatively expressed by Beer Lambert's law, which states that the intensity (I) decays from the original (I_0) according to following equation:

$$I = I_0 e^{-\alpha l c} \tag{7}$$

where, α: absorption coefficient of the material; l: length of travel; c: concentration of the medium. However, there are other factors like scattering, reflection and refraction of light from the bones and skin tissues causing reduction of intensity those are not covered in the law. By convention, the waveform is inverted so that it correlates positively with blood volume [38].

In reflection mode, the source-detector combination is placed on the same side of tissue. In the recent time, green LED operating in 0.5–0.6 μm wavelength has

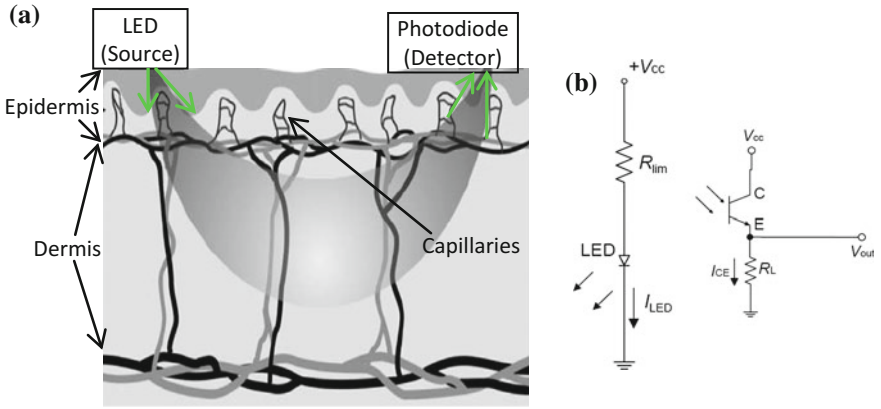

Fig. 11 Photoplethysmography: **a** tissue penetration and backscattering; **b** source and detector circuit configuration

become popular. In this mode, the emitted photons follow banana-shaped path from photodiode to the detector, and barely penetrate deep into the skin [39]. Figure 11a shows the basic principle of reflective PPG sensing.

A typical PPG sensor electronics contains a forward biased LED, producing a light intensity proportional to conductive current with a voltage drop of nearly 2 V across the LED. In Fig. 11b, a current limiting resistance R_{lim} is so chosen that the current (I_{LED}) is sufficient to drive the LED. In the detecting circuit, a load resistor in the phototransistor is used to convert the output current to a voltage as per the following equation:

$$V_L = I_{CE} R_L \tag{8}$$

A typical PPG signal conditioning circuit is shown in Fig. 12 [40]. The total circuit consists of two stages, viz., stage 1 amplifier and filter, and stage 2 amplifiers and filter. The stage 1 and stage 2 are similar in configuration, and use a passive high pass filter of 0.5 Hz and active low pass filter at 3.4 Hz to select the clinical bandwidth of the PPG, which is around 1.5 Hz. The potentiometer P provides an adjustable gain to the final analog output. The reference voltage is kept fixed at 2.0 V. In recent years several wearable PPG sensors have been proposed [41–43].

4.3 Respiration Signal

This section describes the sensor and their interfacing principles for measuring respiration signal using most common methods, viz., differential pressure, thermal convection, microwave Doppler radar, ultrasonic and inductive plethysmography approaches.

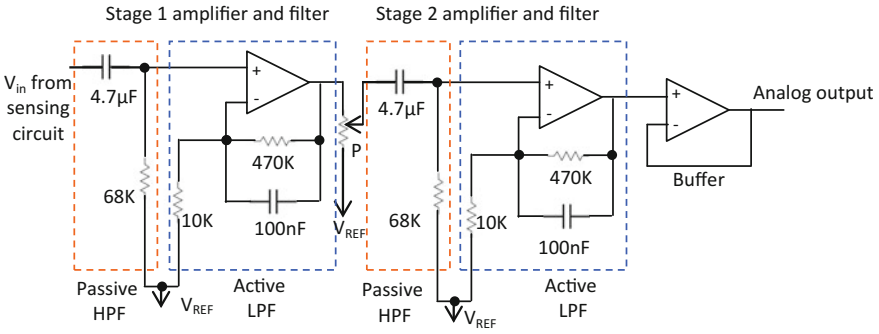

Fig. 12 Signal conditioning of PPG sensor

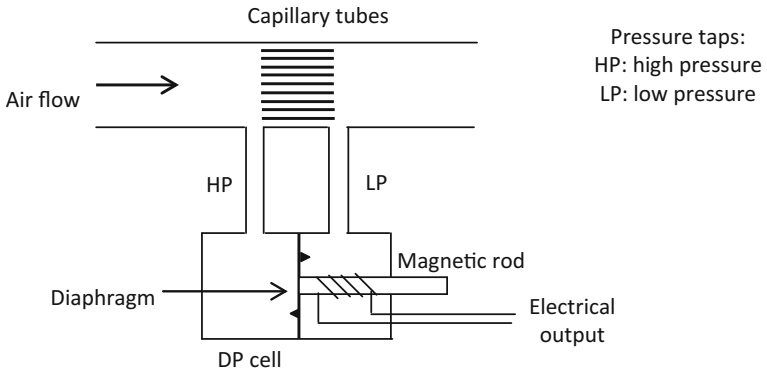

Fig. 13 Schematic of Fleisch pneumotachograph

4.3.1 Differential Pressure (DP) Respiration Sensors

Differential pressure flow meters are one of the oldest and widely used for air flow rate and volume measurement devices. The principle is based on measuring the differential pressure across an element of known resistance, popularly known as pneumotachography. The older version offered by Fleisch is schematically shown in Fig. 13. It provides small capillary tubes as restrictors parallel to the flow line inside the flow conduit. At laminar flow rates, the pressure drop (ΔP) across the restriction is given as:

$$\Delta P = \frac{12\mu l}{\pi N d^4} V \tag{9}$$

Where, d: diameter of each capillary tube, N: Number of tubes; µ: viscosity of the air medium; l: gap between pressure taps; V: flow rate.

The pressure taps (high pressure and low pressure) activate a diaphragm movement in a liquid filled DP cell to generate an electrical output through the displacement of a magnetic plunger rod around which a coil is wound to form an electromagnetic transducer. A modified version, named screen pneumotachograph, uses fine wire mesh replacing the capillary tubes. Both versions have flat frequency response up to 20 Hz but sensitive to changes in temperature, humidity, and gas composition [19]. A variable orifice type flow meter uses almost same principle and overcome with the additional advantage of handling turbulent flow [44].

4.3.2 Thermal Convection Type Respiration Sensors

Hot wire anemometers are the most popular type air flow measurement systems used in commercial systems under clinical setting. A typical configuration is shown in Fig. 14a. A heated wire is mounted perpendicular to the flow line (nasal cavity or mouth) in a tapered tube and constitutes one arm of a full Wheatstone bridge. The heater element is maintained at constant temperature. The airflow due to breathing takes away the heat from the sensing element. In signal conditioning circuit, shown in Fig. 14b, the bridge unbalance voltage is fed to a high gain DC amplifier and an emitter follower stage [45]. The current drawn from the source to maintain the constant temperature of sensor wire can be used to measure the volumetric flow rate.

A convective heat transfer based sensor design for neonatal ventilation system is proposed in [46]. Two electrically heated transistor elements (T_1 and T_2), mounted on separate circuit boards (c_1 and c_2) flushed into the flow pipe and held perpendicular to the air flow is used as sensor assembly, as shown in Fig. 15a. The circuit boards are held at a small gap, with sensing elements mounted on opposite faces, thus thermally insulating them. Each transistor is used in common-emitter configuration and supplied with constant current. Thus, the heat taken away by the cold (er) air will be different for each sensor in bidirectional flow (inspiration and

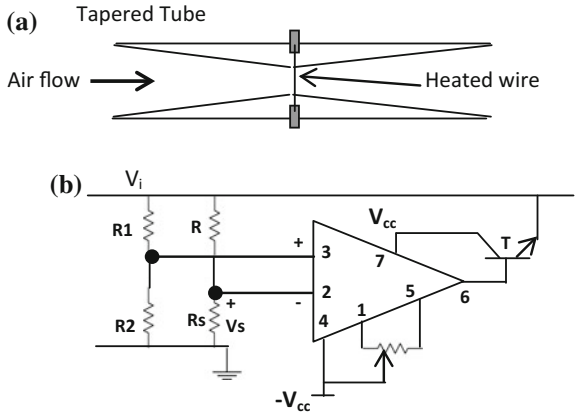

Fig. 14 Hot wire anemometer: **a** Sensor configuration and **b** interfacing circuit

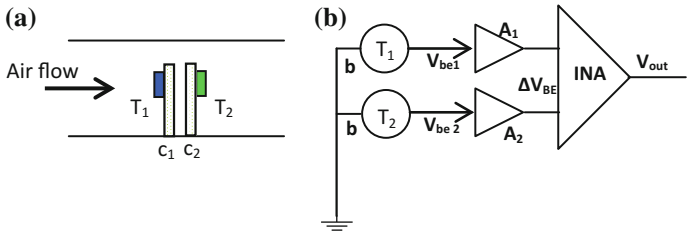

Fig. 15 Thermal convection type respiration sensing using differential heating of transistors: **a** Sensor mounting. **b** Signal conditioning schematic

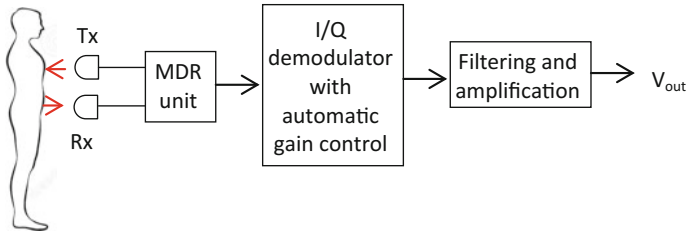

Fig. 16 Typical test set up of a MDR system for respiration measurement

expiration cycle). The signal conditioning circuit as shown in Fig. 15b, utilizes the difference in base-emitter voltage of two transistors through first stage and INAs to get the final analog output (V_{out}). Another silicon based thermal convection type respiration measurement unit is described in [47].

4.3.3 Microwave Doppler Radar (MDR) Type Respiration Sensors

A typical MDR system employs a pair of transmit and receive antenna mounted close to the body of the subject and captures the frequency shift of the reflected wave from the target (chest or abdomen) based on its quasi periodic motion due to respiration. The theoretical analysis [23] shows that the inhalation, exhalation and the pause in between them can be represented as a phase modulated signal, with the phase shift directly proportional to the object's chest movement.

A typical test-set up with interfacing schematic is shown in Fig. 16. A pair of Tx-Rx antenna transmits and receives the frequency modulated CW microwave radiation in the GHz range (based on antenna size), controlled by the MDR unit. The received signal is passed through a direct quadrature demodulator with RF and baseband automatic gain control, facilitating quadrature demodulation into direct baseband frequencies [48]. The final output is low pass filtered (with amplifiers) to extract the respiration signal V_{out} [49, 50].

4.3.4 Ultrasonic Respiration Meters

Ultrasonic respiration sensors can either use Doppler effect, i.e., change in frequency or phase shift of the reflected signal based on quasi-periodic motion of the chest due to respiration [51], or use transit time principle. A piezo crystal operating at 40 kHz frequency transmits short bursts of ultrasonic wave to the target (human chest), which reflects back the pulses to the receiver. The receiver calculates the time of travel, considering the speed of sound wave in the medium (air). The resolution in measurement can be improved with higher frequency. However, direct time of flight measurements suffer from the inaccuracies that occur in measurement of the flight time (~μs or less), and inertial delay problem in piezo sensor. To counteract these, envelope detection principle is used in [52, 53]. This provides an indirect measurement of time-of-flight of the pulses. A typical configuration is shown in Fig. 17.

The transceiver is placed near to the body, typically within 100 cm to avoid heavy attenuation of reflected wave energy. The reflected signal is passed through an amplifier, an envelope detector and a band pass filter to extract the low frequency respiration information. An envelope detection circuit detects the peaks from the amplitude modulated high frequency signals at the output of amplifier. Finally, the analog output is digitized and collected in a personal computer.

4.3.5 Respiratory Inductive Plethysmography (RIP) Sensors

The common RIP sensor consists of an elastic chest and abdomen belt (around 1 inch wide) with a zigzagging wire sewn into it and worn around the chest (rib cage under the armpits) and abdomen. A small current (some 10–20 mA) is passed through the coil from an oscillator. During inspiration, the abdomen (rib cage) area decreases (increases) with the lung volume. A typical RIP configuration is shown in Fig. 18. The outputs of the sensing units are separately amplified, and filtered to extract the respiration information before being added. Since the amplitudes of abdomen and chest sensors are unequal, the outputs of filters are normalized before addition.

An improved version of RIP sensor [54] uses pulsed current excitation (15 mA at 400 kHz for 100 μs) in time division multiplexing (TDM) to activate multiple

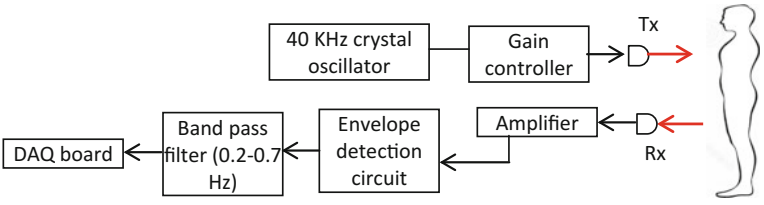

Fig. 17 Ultrasonic respiration measurement schematic

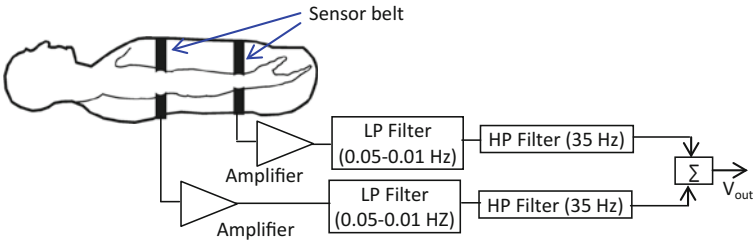

Fig. 18 Basic RIP sensor configuration and signal conditioning

sensors controlled by CMOS switching circuit. For sensing, a parallel LC circuit is used with a fixed C and L being the loop wire inductance. This combination virtually acts as a band pass filter with variable central frequency, which changes the output amplitude as per change in inductance due to breathing. Thus voltage change across the sensing unit can be detected to reflect the respiration rate.

4.4 Blood Pressure Signal

This section briefly describes the sensor interfacing for catheter type electrical blood pressure sensors. The most common configuration involves an elastic member (diaphragm) to be deflected by the blood pressure. The different secondary sensing principles can be categorized into the following.

4.4.1 Capacitive Blood Pressure Sensors

The displacement of the elastic diaphragm can be utilized to form a variable capacitance transducer, using the diaphragm with a thin conductive coating as movable plate. For a circular diaphragm fixed at the periphery, the approximate deflection (y) at the centre is given as:

$$y = \frac{3PR^4\left[\left(\frac{1}{\sigma}\right)^4 - 1\right]}{16E\left(\frac{1}{\sigma}\right)^2\delta^3} \tag{10}$$

where, E: Young's modulus of the material, σ: Poisson's ratio, P: applied pressure, δ: thickness of the diaphragm, R: radius of the diaphragm.

The sensor structure and lead connectors are encapsulated in a small volume by macro machining technique to achieve a sensor dia of 500 μm, diaphragm thickness and plate gap of 1 μm each, giving a capacitance value of 3 pF [55]. The problems encountered with this type of sensors are higher inherent electrical noise,

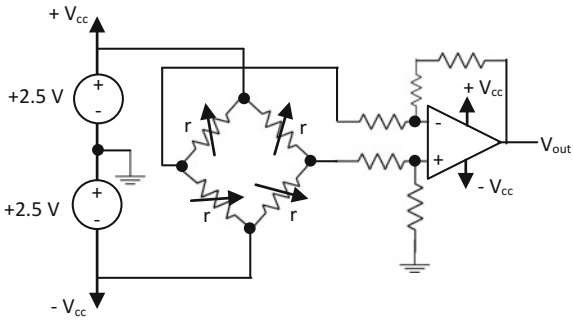

Fig. 19 Typical signal conditioning circuit of piezoresistive BP sensor

requirement of complex signal processing, internal oscillator and demodulator, which also increases the overall cost.

In another configuration [56], the variable capacitance is realized in a FET structure, so that, with the movement of the diaphragm reduces the gate and source resistance and source-drain current is altered.

4.4.2 Piezoresistive Blood Pressure Sensors

A four arm Wheatstone bridge is used with four active resistive elements each connected to one arm; with two in compression mode and the rest in expansion mode. Common piezoresistive transducers are ion-implanted into a thin silicon monocrystalline membrane [56, 57]. Typical values are 100–3 kΩ and powered by 3 V. The output (v_0) of the four-arm Wheatstone bridge excited by supply v_s is obtained as,

$$v_0 = v_s \frac{\Delta r}{r} \tag{11}$$

where, Δr/r is the fractional change in resistance, assumed to be equal in each piezoresistive arms. The schematic circuit diagram is shown in Fig. 19. The bridge output is fed to an INA, followed by a successive approximation type AD converter.

4.4.3 Optical Blood Pressure Sensors

Their most advantageous feature is use of an optical beam, thus the risk of inducing current to the patient body is avoided, along with decoupling of associated electronics at the sensor site. The basic principle of sensing can be divided into the following categories: (a) Intensity reflective fiber optic sensor; (b) light coupling between two fiber optic sensors, (c) microbending fiber optic sensor, and (d) fiber optic sensing based on interferometer principles. The most straightforward

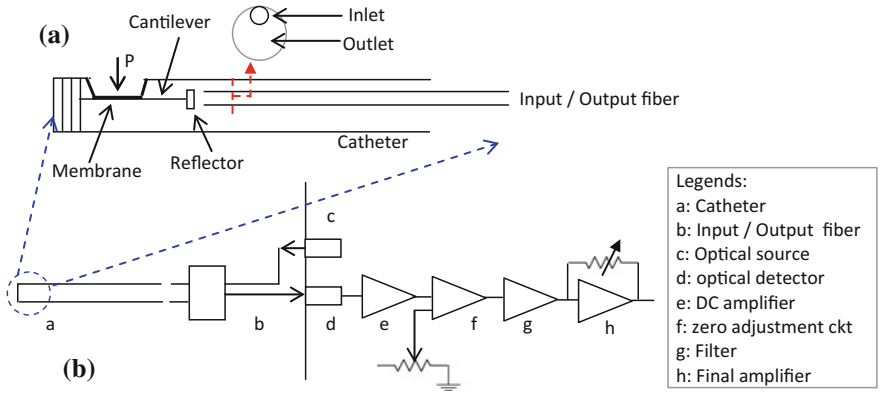

Fig. 20 **a** Schematic configuration and **b** signal conditioning of FO cantilever pressure catheter sensor

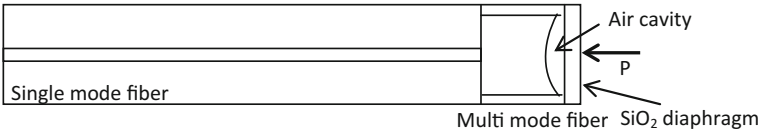

Fig. 21 Schematic blood pressure sensor using FP interferometry

configuration uses passing or reflecting light beam through the deflection system (elastic member) [58, 59] and measures the modulation by an electronic circuit. A classical configuration of a cantilever fiber optic catheter probe is shown in Fig. 20a. A cantilever arrangement accepts the pressure on a membrane coupled to a reflector, which faces the single Fiber cable acting as inlet and outlet and guides the light pulses to the catheter tip. A change in pressure alters the amount of reflected light into the output fiber. The modulation in light intensity is sensed by a photo electric detector and the final output is filtered, amplified to get a scaled output. The signal conditioning schematic is shown in Fig. 20b.

In another configuration [60] a Fabry-Perot (FP) interferometry is described to measure aortic arch and right coronary artery pressure. As shown schematically in Fig. 21, it consists of a single mode fiber, a multi-mode fiber, and a SiO_2 diaphragm. The SiO_2 diaphragm couples the pressure (P) at the catheter tip. An FP cavity is formed by multi-mode fiber—air cavity interface and air cavity—diaphragm interface. The single mode fiber guides the light exciting on the FP cavity and collects the reflected light. The multiple reflections of light in the FP cavity form an interference pattern.

The change in pressure on the diaphragm alters the FP cavity length and this is reflected in the phase change of the interference pattern. This in turn brings sinusoidal changes the intensity of the final reflected optical beam. The reflected light can be split into two fibers using an optical splitter, one directly connected to an

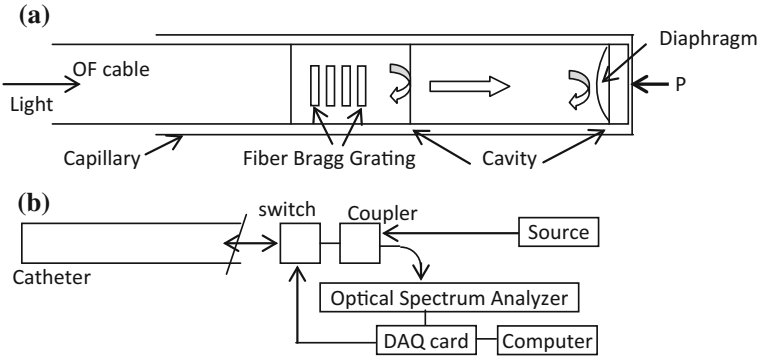

Fig. 22 **a** Schematic of fiber bragg grating type FP interferometric BP sensor. **b** Measurement set up

optical detector (broadband channel) and the other via a tunable filter (narrowband channel). The difference in pattern between the two detectors can be mathematically correlated to the blood pressure.

A temperature compensated extrinsic fiber optic interferometer BP sensor is schematically presented in Fig. 22. It contains an integrated fiber Bragg grating (FBG) core by periodic change in the refractive index inside a single mode fiber. The fiber is drawn into a glass capillary, at the end of which a diaphragm is sealed by splicing a multimode, which accepts the blood pressure. A FP cavity is formed between the diaphragm and the FBG which facilitates reflection of light. The outside pressure can change the cavity length (ΔL) through deformation of the diaphragm, calculated as in [61]:

$$\Delta L = \frac{3}{16}\frac{(1-\mu^2)}{E}\frac{r^4}{h^3}\Delta P \tag{12}$$

The measurement set-up consists of an optical source, coupler with switch (operating in time multiplexing mode and controlled by DAQ card), an optical spectrum analyzer (OSA), data acquisition card and computer. The coupler directs the light pulses from sources and redirects the reflected light into the receiver fiber. The OSA converts the received radiation into intensity modulated electrical pulses, which are finally analysed in the computer.

4.4.4 Oscillometric Blood Pressure Sensor

Most of the automatic BP monitors use the principle of oscillometry, where the oscillations in occluded cuff pressure with gradual release of cuff pressure is sensed by peizoresistive sensors connected in a Wheatstone bridge. The bridge output is filtered, amplified and processed by a microcontroller to compute the systolic,

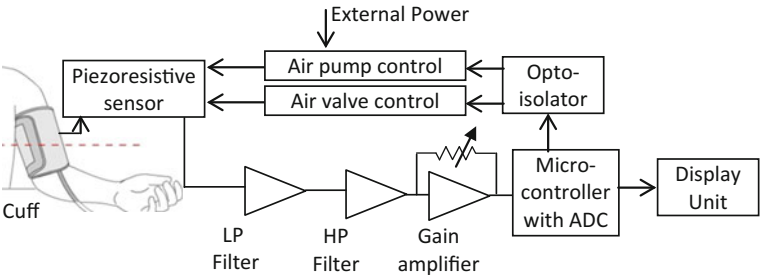

Fig. 23 Block schematic of an automatic BP monitor using oscillometry

diastolic and mean arterial pressures (MAP). Figure 23 describes a schematic layout of such a system. The air cuff is provided with a controlled air supply and air valve control system, both controlled from a central microcontroller. The sensor output is typically filtered by a series of low pass (10 Hz) and high passes (2.2 Hz) filters and a gain control stage to generate an analog output that is fed to the microcontroller unit. The microcontroller determines the MAP by taking the cuff pressure when the pulse with the largest amplitude appears. Typically, in some commercial units [62] calculates the systolic pressure (diastolic pressure) equal to the measurement taken in the cuff with a pulse with 70% (50%) of the amplitude of the MAP while the cuff pressure is above (below) the MAP value.

5 Wireless Biomedical Instrumentation

With the advent of low power microelectronics, embedded systems, sensing technology and wireless communication techniques, the area of medical instrumentation has undergone sea change in the last two decades. Using miniature wearable sensors with digital intelligence, a patient's medical condition can be remotely monitored under his normal activity. Development of low power hungry digital microcontrollers has enabled fast real-time analysis of the acquired signals for conditioning monitoring of critical patients. Hence, modern biomedical instrumentation systems are not only confined to measurement, and acquisition of data, but include significant computing tasks for analyzing the acquired signals [63]. Over the last decade, low power industrial, scientific and medical (ISM) band protocols (ZigBee, WLAN and Bluetooth) have been widely used in short range health monitoring applications [64–66].

A typical configuration of multi (two)-channel wireless biomedical instrumentation system is shown in Fig. 24. The hardware acquisition module (HAM) is a small circuit encompassing the signal conditioning functions and digital interface to transfer the signals through a wireless media to handheld gadgets, or remote servers. The HAM includes a low power microcontroller which controls the

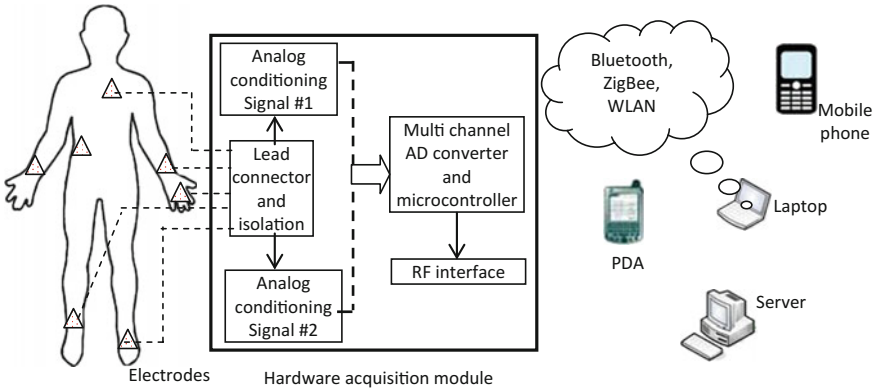

Fig. 24 Block schematic of a typical multi-channel wireless biomedical signal acquisition system

multiplexing of the conditioned signals and transfers the data using a serial protocol to the on-board RF interfaces. For short distance monitoring, these RF modules utilize license free ISM bands and comply with either ZigBee or Bluetooth or WLAN protocol. For remote-end connectivity, all the sensors' data is routed through a gateway to a public communication network (PSTN, internet or ISDN etc.). Now a days, a variety of low power RF modules are commercially available in the consumer market, which can be used to develop custom make health monitoring applications [67]. Body area network (BAN), a specialized application of sensor network has enabled wireless networking among various sensors attached to different parts of the body using dedicated wireless protocols (medical implant communication service, MICS, at 402–405 MHz and wireless medical telemetry services, WMTS at 608–614 MHz).

6 Trends in Biomedical Sensor Technology

Considering the huge potential of biomedical science and healthcare in the coming days, the following developments are expected to play key roles in medical instrumentation domain.

6.1 Use of Wearable Integrated Biomedical Sensors

With the increasing demand from the patients to stay in normal life while being monitored for their physiological activity, wearable biomedical sensors can play an

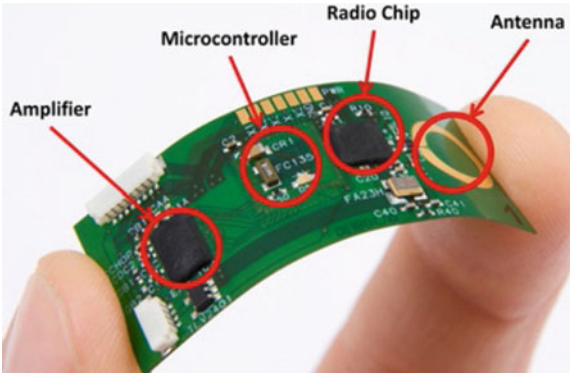

Fig. 25 Flexible integrated ECG sensor from IMEC, Netherlands

important role. Towards this objective, new adhesive tape type wearable sensors enable integration of sensors, signal conditioning, digitization, controller, energy source (collector) and low power RF module in a small area (less than 2 sq. inch) and fixed on human body [68, 69]. Figure 25 shows the diagram of a flexible ECG sensor which contains three electrodes, an amplifier, microcontroller and RF chip and transceiver units on small flexible polymer strip.

The design challenges for these units are low power consumption, ease of wearing, and energy harvesting for continuous data supply.

6.2 Context Aware Smart Biomedical Sensors

For continuous monitoring of patients in their normal activity, an important requirement is real-time recognition of abnormal 'events' (fall, unconsciousness etc.) which can be communicated to a caregiver. Autonomous sensor systems, as described in last section lack in computational capability due to small size of the embedded processor. However, such smart capability can be achieved in conjunction with a device with higher computational capability, typically a mobile phone or PDA which the patient often carries. The software in the device can be intelligent enough to discriminate a normal and abnormal condition, however, in such systems additional sensors (like accelerometers, temperature sensors) may be deployed.

Acknowledgements The author would like to Mrs. Priyanka Bera, research scholar at Department of Applied Physics, University of Calcutta, India for the help in copyediting and proof reading of the manuscript.

References

1. R. Plonsey, R.C. Barr, *Bioelectricity: A Quantitative Approach*, 3rd edn. (Springer, NY, USA, 2007)
2. J.D. Bronzino (ed.), *The Biomedical Engineering Handbook*, 2nd edn. (CRC Press LLC, Boca Raton, USA, 2000)
3. L.A. Geddes, L.E. Baker, *Biopotential and Electrophysiology Measurement*
4. J.G. Webster (ed.), *Medical Instrumentation: Application and Design*, 4th edn. (Wiley, USA, 2010)
5. A. Natale, F. Marchlinski (ed.), *Handbook of Cardiac Electrophysiology* (Informa Healthcare, CRC Press, Boca Raton, USA, 2007)
6. F. Morris, W.J. Brady, J. Camm (eds.), *ABC of Clinical Electrocardiography* (BMJ Publishing, USA, 2008)
7. L. Schamroth, C. Schamroth, *An introduction to Electrocardiography*, 7th edn. (Blackwell Science, France, 2008)
8. R. Gupta, M. Mitra, J.N. Bera, *ECG Acquisition and Automated Remote Processing* (Springer, India, 2014)
9. A.B. Hertzman, The blood supply of various skin areas as estimated by the photoelectric plethysmograph. Am. J. Physiol. **124**, 328–340 (1938)
10. A.A.R. Kamal, J.B. Harness, G. Irving, A.J. Mearns, Skin photoplethysmography—a review. Comput. Methods Programs Biomed. **28**(4), 257–269 (1989)
11. J. Allen, Photoplethysmography and its application in clinical physiological measurement. Physiol. Meas. **28**(2007), R1–39 (2007)
12. S.C. Millasseau, R.P. Kelly, J.M. Ritter, P.J. Chowienczyk, Determination of age-related increases in large artery stiffness by digital pulse contour analysis. Clin. Sci. 371–377 (2002)
13. E. Tam et al., Correction of cardiac output obtained by modelflow® from finger pulse pressure profiles with a respiratory method in humans. Clin. Sci. 371–376 (2014)
14. P. Wang, W. Zuo, D. Zhang, A compound pressure signal acquisition system for multichannel wrist pulse signal analysis. IEEE Trans. Instrum. Meas. **63**(6), 1556–1565 (2014)
15. Y Kurylyak, K. Barbe, F. Lamonaca, D. Grimaldi, W. Van Moer, Photoplethysmogram-based blood pressure evaluation using Kalman filtering and NN, in *Proceedings of International Symposium on Medical Measurements and Applications (MeMeA)*, May 3–4 (2013), pp. 170–174
16. L. Nilsson, A. Johansson, S. Kalman, Respiratory variations in the reflection mode photoplethysmographic signal: relationships to peripheral venous pressure. Med. Biol. Eng. Comput. **41**(3), 249–254 (2003)
17. R. Erts, E. Kviesis-Kipge, J. Zaharans, E. Zaharans, J. Spigulis, Wireless photoplethysmography finger sensor probe, in *Proceedings of 12th Biennial Baltic Electronics Conference (BEC2010)*, Tallinn, Estonia, October 4–6 (2010), pp. 283–284
18. E.M. Lee, J.Y. Shin, J.H. Hong, E.J. Cha, T.S. Lee, Glass-type wireless PPG measuring system, in *32nd. Annual International Conference of the IEEE EMBS*, August 31–September 4 (2010), pp. 1433–1436
19. J.G. Webster (ed.), *The Physiological Measurement Handbook* (CRC Press, USA, 2015)
20. S. Silvestri, E. Schena, Micromachined flow sensors in biomedical applications. Micromachines **3**, 225–243 (2012)
21. Y.S. Lee, P.N. Pathirana, C.L. Steinfort, T. Caelli, Monitoring and analysis of respiratory patterns using microwave doppler radar. IEEE J. Trans. Eng. Health Med. **2** (2014)
22. C. Gu, C. Li, Assessment of human respiration patterns via noncontact sensing using doppler multi-radar system. Sensors **15**(3), 6383–6398 (2015)
23. Y.S. Lee, P.N. Pathirana, R.J. Evans, C.L. Steinfort, Noncontact detection and analysis of respiratory function using microwave doppler radar. J. Sens. 1–13 (2015)
24. G.D. Garguilo et al., A wearable contactless sensor suitable for continuous simultaneous monitoring of respiration and cardiac activity. J. Sens. 1–6 (2015)

25. S.T.A. Hamdani, A. Fernando, The application of a peizo-resistive cardiorespiratory sensor system in an automobile safety belt. Sensors **15**(4), 7742–7753 (2015)
26. Z. Zhang et al., Development of respiratory inductive plethysmography module supporting multiple sensors for wearable systems. Sensors **12**(10), 13167–13184 (2012)
27. K. Konno, J. Mead, Measurement of the separate volume changes of rib cage and abdomen during breathing. J. Appl. Physiol. **22**(3), 407–422 (1967)
28. L.A. Geddes, *Handbook of Blood Pressure Measurement* (Springer Science Business Media, NY, 1991)
29. J.G. Webster (ed.), *The Measurement, Instrumentation and Sensors Handbook* (CRC Press LLC, USA, 1999)
30. J.S. Kim, Y.J. Chee, J.W. Park, J.W. Choi, K.S. Park, A new approach for non-intrusive monitoring of blood pressure on a toilet seat. Physiol. Meas. **27**(2), 203–211 (2006)
31. M. Nitzan, A. Patron, Z. Glik, A.T. Weiss, Automatic noninvasive measurement of systolic blood pressure using PPG. Biomed. Eng. Online 1–8 (2009)
32. J.H. Shin, K.M. Lee, K.S, Park, Non-constrained monitoring of systolic blood pressure on a weighing scale. Physiol. Meas. **30**, 679–693 (2009)
33. M. Mukkamala et al., Toward ubiquitous blood pressure monitoring using pulse transit time theory and practice. IEEE Trans. Biomed. Eng. **62**(8), 1879–1901 (2015)
34. D. Buxi, J.M. Redoute, M.R. Yuce, A survey on signals and systems in ambulatory blood pressure monitoring using pulse transit time. Physiol. Meas. **36**(3), R1–R26 (2015)
35. R.B. Northorp, *Analysis and Application of Analog Electronic Circuits to Biomedical Instrumentation*, 2nd edn. (CRC Press, Boca Raton, USA, 2012)
36. M. Degrauwe, I. Verbauwhede, A micropower CMOS-instrumentation amplifier. IEEE J. Solid State Circ. **Cs-20**(3), 805–807 (1985)
37. E.M. Spinelli, R.P. Areny, M.A. Mayosky, AC-coupled front-end for biopotential measurements. IEEE Trans. Biomed. Eng. **50**(3), 391–395 (2003)
38. A. Reisner, P.A. Shaltis, D. McCombie, H.H. Asada, Utility of the photoplethysmogram in circulatory monitoring. Anesthesiology **108**, 950–958 (2008)
39. T. Tamura, Y. Maeda, M. Sekine, M. Yoshida, Wearable photoplethysmographic sensors—past and present. Electronics **3**(2), 282–302 (2014)
40. Easy Pulse PPG sensor from Embedded Lab, http://www.embedded-lab.com
41. S. Borik, I. Cap, Implementation of wireless data transfer to photoplethysmographic measurements. Proc. ElEKTRO **21–22**, 407–410 (2012)
42. G. Angius, L. Raffo, Cardiovascular disease and sleep apnoea: a wearable device for PPG acquisition and research aims, in *Proceedings of Computing in Cardiology*, 9–12 September (2012), pp. 513–516
43. K. Davoudi, M. Shayegannia, B. Kaminska, Vital signs monitoring using a new flexible polymer integrated PPG sensor. Proc. Comput. Cardiol. **22–25**, 265–268 (2013)
44. G. Tardi, C. Massaroni, P. Saccomandi, E. Schena, Experimental assessment of a variable orifice flowmeter for respiratory monitoring. J. Sens. 1–8 (2015)
45. G.A.L. Araujo, R.C.S. Freire, J.F. Silva, A. Oliveira, E.F. Jaguaribe, Breathing flow measurement with constant temperature hot wire anemometer for forced oscillations technique, *in Proceedings of instrumentation and measurement technology conference*, Italy, Vol. 1, May (2004), pp. 730–733
46. M. Giorgino et al., Design and characterization of a bidirectional low cost flowmeter for neonatal ventilation. IEEE Sens. J. **14**(12), 4354–4360 (2014)
47. M.J.A.M. van Putten, M.H.P.M. van Putten, A.F.P. van Putten, J.C. Pompe, H.A. Bruining, A silicon bidirectional flow sensor for measuring respiratory flow. IEEE Trans. Biomed. Eng. **44** (2), 205–208 (1997)
48. AD8347 Direct Conversion Quadrature Demodulator Datasheet, http://www.analog.com
49. O. Postolache, P.S. Girao, E. Lunca, P. Bicleaknu, Unobtrusive cardio-respiratory monitoring based on microwave doppler radar, in *Proceedings of 2012 International Conference and Exposition on Electrical and Power Engineering (EPE 2012)*, 25–27 October, Iasi, Romania (2012), pp. 597–600

50. M. Zakrzewski, A. Vehkaoja, A.S. Joutsen, K.T. Palovuori, J.J. Vanhala, Noncontact respiration monitoring during sleep with microwave doppler radar. IEEE Sens. J. **15**(10), 5683–5693 (2015)
51. P. Arlotto, M. Grimaldi, R. Naeck, J.M. Ginoux, An ultrasonic contactless sensor for breathing monitoring. Sensors **14**, 15371–15386 (2014)
52. Yusuke Yamana, et al., A sensor for monitoring pulse rate, respiration rhythm, and body movement in bed, in *Proceedings of 33rd Annual International Conference of the IEEE EMBS*, Boston, Massachusetts USA, August 30–September 3 (2011), pp. 5323–5326
53. S.D. Min, Noncontact respiration rate measurement system using an ultrasonic proximity sensor. IEEE Sens. J. **10**(11), 1732–1739 (2010)
54. Z. Zhang et al., Development of a respiratory inductive plethysmography module supporting multiple sensors for wearable systems. Sensors **12**, 13167–13184 (2012)
55. K.E. Babbitt, L. Fuller, B. Keller, A surface micromachined capacitive pressure sensor for biomedical applications, in *Proceedings of the Twelfth Biennial University/Government/ Industry Microelectronics Symposium*, 20–23 July (1997), pp. 150–153.
56. Samaun, K.D. Wise, J.B. Angell, An IC Piezoresistive Pressure Sensor for Biomedical Instrumentation. IEEE Trans. Biomed. Eng. **BME-20**(2), 101–109 (1973)
57. M. Esashi et al., Fabrication of catheter-tip and sidewall miniature pressure sensors. IEEE Trans. Electron Devices **-ED-39**(1), 57–63 (1982)
58. H. Matsumoto, M. Saegusa, K. Saito, K. Mizoi, The development of a fibre optic catheter tip pressure transducer. J. Med. Eng. Technol. **2**(5), 239–242 (1978)
59. A. Lekholm, L. Lindström, Optoelectronic transducer for intravascular measurements of pressure variations. Med. Biol. Eng. **7**, 333–335 (1969)
60. N. Wu et al., A miniature fiber optic blood pressure sensor and its application in vivo blood pressure measurements of a swine model. Sens. Actuators B: Chem. **181**, 172–178 (2013)
61. S. Poeggel, D. Tosi, G. Leen, E. Lewis, Low drift and high resolution miniature optical fiber combined pressure—and temperature sensor for cardio-vascular and other medical applications, in *Proceedings of the 2013 IEEE Sensors*, Baltimore, MD, USA, 3–6 November (2013), pp. 1–4
62. S. Lopez, *Blood Pressure Monitor Fundamentals and Design* (Freescale Semiconductor Application Note)
63. H. Eren, J.G. Webster (eds.), *Telemedicine and Electronic Medicine* (CRC Press, Boca Raton USA, 2015)
64. S.K. Chen et al., A reliable transmission protocol for zigbee-based wireless patient monitoring. IEEE Trans. Inf Technol. Biomed. **16**(1), 6–16 (2012)
65. H.J. Lee et al., Ubiquitous health care service using zigbee and mobile phone for elderly patients. Int. J. Med. Inf. **78**(3), 193–198 (2009)
66. R. Gupta, J.N. Bera, M. Mitra, An intelligent telecardiology system for offline wireless transmission and remote analysis of ECG. J. Med. Eng. Technol. (Informa Healthcare) **36**(7), 358–365 (2012)
67. S. Roy, R. Gupta, Short range centralized cardiac health monitoring system based on zigbee communication, in *2014 IEEE Global Humanitarian Technology Conference (GHTC)-South Asia Satellite*, September 26–27, 2014, Kerala, India (2014), pp. 177–182
68. S. Patel, H. Park, P. Bonato, L. Chan, M. Rodgers, A review of wearable sensors and systems with application in rehabilitation. J. NeuroEng. Rehabil. **9**(21), 1–17 (2012)
69. L.G. Villanueva, S. Cagnoni, L. Ascari, Design of a wearable sensing system for human motion monitoring in physical rehabilitation. Sensors **13**, 7735–7755 (2013)